butadiene or the Claisen rearrangement readily come to mind in this context.

REFERENCES AND NOTES

1. R. Wyler, J. de Mendoza, J. Rebek Jr., *Angew. Chem. Int. Ed. Engl.* **32**, 1699 (1993); N. Branda, R. Wyler, J. Rebek Jr., *Science* **263**, 1267 (1994).
2. R. Meissner, J. Rebek Jr., J. de Mendoza, *Science* **270**, 1485 (1995).
3. C. T. Seto, and G. M. Whitesides, *J. Am. Chem. Soc.* **113**, 712 (1991); M. Simard, D. Su, J. D. Wuest, *ibid.*, p. 4696; P. Baxter, J.-M. Lehn, A. DeCian, J. Fischer, *Angew. Chem. Intl. Ed. Engl.* **32**, 69 (1993); R. P. Bonar-Law and J. K. M. Sanders, *Tetrahedron Lett.* **34**, 1677 (1993); M. R. Ghadiri, J. R. Granja, R. A. Milligan, D. E. McRee, N. Khazanovich, *Nature* **366**, 324 (1993); J. Yang, E. Fan, S. J. Geib, A. D. Hamilton, *J. Am. Chem. Soc.* **115**, 5314 (1993); M. R. Ghadiri, K. Kobayashi, J. R. Granja, R. K. Chadha, D. E. McRhee, *Angew. Chem. Intl. Ed. Engl.* **34**, 93 (1995); J. P. Mathias, C. T. Seto, E. E. Simanek, G. M. Whitesides, *J. Am. Chem. Soc.* **116**, 1725 (1994); J. P. Mathias, E. E. Simanek, J. A. Zerkowski, C. T. Seto, G. M. Whitesides, *ibid.*, p. 4316; J. P. Mathias, E. E. Simanek, G. M. Whitesides, *ibid.*, p. 4326.
4. C. Valdés, U. P. Spitz, S. W. Kubik, J. Rebek Jr., *Angew. Chem. Int. Ed. Engl.* **34**, 1885 (1995).
5. R. G. Chapman and J. C. Sherman, *J. Am. Chem. Soc.* **117**, 9081 (1995).
6. Because there is competition between the solute and solvent molecules for occupancy of the cavity, the encapsulation of a desired guest molecule can be encouraged by the use of a solvent that is larger than the cavity can comfortably accommodate. This tactic has been developed for carcerands and other synthetic receptors [M. L. C. Quan and D. J. Cram, *J. Am. Chem. Soc.* **113**, 2754 (1991); K. T. Chapman and W. C. Still, *ibid.* **111**, 3075 (1989)].
7. The energy-minimized structure was obtained with the program MacroModel 3.5X on a Silicon Graphics Personal Iris workstation.
8. A. I. Vogel, *Vogel's Textbook of Practical Organic Chemistry* (Longman, Essex, ed. 5, 1989), pp. 939–940.
9. K. D. Bartle, H. Heaney, D. W. Jones, P. Lees, *Tetrahedron* **21**, 3289 (1965).
10. N. Branda, R. M. Grotzfeld, C. Valdés, J. Rebek Jr., *J. Am. Chem. Soc.* **117**, 85 (1995).

11. The authors are grateful to the National Institutes of Health for financial support. We thank U. P. Spitz for assistance with the ^{13}C NMR experiments and B. O'Leary for assistance with the synthesis of precursor compounds.

15 August 1995; accepted 21 November 1995

Design of a Random Quantum Spin Chain Paramagnet: $Sr_3CuPt_{0.5}Ir_{0.5}O_6$

Tu N. Nguyen, Patrick A. Lee, Hans-Conrad zur Loye*

A new class of magnetic behavior, random quantum spin chain paramagnetism, has been observed in the one-dimensional compound $Sr_3CuPt_{1-x}Ir_xO_6$. A random quantum spin chain system has $S = ½$ spins coupled by Heisenberg exchange interactions that are randomly ferromagnetic or antiferromagnetic between neighbors along the chain. This condition was fulfilled by members of the solid solution $Sr_3CuPt_{1-x}Ir_xO_6$ ($x = 0$, 0.25, 0.50, 0.75, and 1), whose end-members, Sr_3CuPtO_6 and Sr_3CuIrO_6, are antiferromagnetic and ferromagnetic, respectively. Magnetic susceptibility data for the solid solution $Sr_3CuPt_{1-x}Ir_xO_6$ ($x = 0$, 0.25, 0.50, 0.75, and 1) were collected and were found to be in excellent agreement with a theoretical model.

Low-dimensional materials, both one- and two-dimensional (1D and 2D), have long been of interest to chemists and physicists because of their distinctive electronic and magnetic properties. The strong directionality of low-dimensional structures can produce highly anisotropic physical properties because interactions between electrons, such as magnetic coupling, can depend strongly on the crystallographic directions along which they occur. A wide variety of interesting phenomena have been observed in low-dimensional solids. Some examples are the appearance of the Haldane gap in Heisenberg chains with integer spins (*1*), the observation of the spin–Peierl's transition in linear Cu^{2+} chains in the inorganic compound $CuGeO_3$ (*2*) and in the organic bis-(dithiolene)-copper-tetrathiafulvalene complex (*3*), the existence of 1D antiferromagnetic ordering in tetramethyl ammonium manganese chloride (TMMC) (*4*) and in dichloro-bis(pyridine) copper(II) (CPC) (*4*), and the observation of 1D random antiferromagnetic exchange in the $S = ½$ salt quinolinium tetrathiafulvalene (*5*).

Random 2D and 3D spin systems have been studied extensively. At low temperatures, they generally form spin glasses, in which the spins freeze into an infinite variety of ground states because of the frustration generated by the random exchange. In a 1D spin chain, however, frustration does not occur. The ground state is unique: Each spin can point in a direction such that the exchange energy with both its neighbors, whatever its sign, is minimized. This picture describes correctly the ground state of the random classical spin chain, and its entropy at finite temperatures is the same as that of a ferromagnetic chain, which has been solved exactly (*6*). However, when the quantum mechanical nature of the spin is taken into account, and $S = ½$ is the case where quantum effects are most important, the nature of the ground state and its low-lying excitations is not at all obvious. The random $S = ½$ chain with purely antiferromagnetic but random exchange has been studied, both experimentally (*5*) and theoretically (*7*, *8*). We have found, however, that the existence of exchange interactions of both signs changes the nature of the states qualitatively. A recent renormalization group analysis (*9*) shows that the case with both signs of exchange belongs to a new universality class, so that the low-temperature behavior is expected to be quite different. Here, we report on a new class of 1D compounds, random quantum spin chains, that consist of $S = ½$ spins coupled by Heisenberg exchange interactions that are randomly ferromagnetic or antiferromagnetic.

We synthesized and characterized a 1D system that exhibits random quantum spin chain paramagnetism, a magnetic phenomenon that can occur in 1D chains that exhibit random ferromagnetic and antiferromagnetic coupling within the chains. The theory developed by Furusaki *et al.* (*10*), which explains the magnetic data of such 1D materials, prompted us to attempt this synthesis. We had been investigating a series of 1D oxides, $Sr_3MM'O_6$ (Figs. 1 and

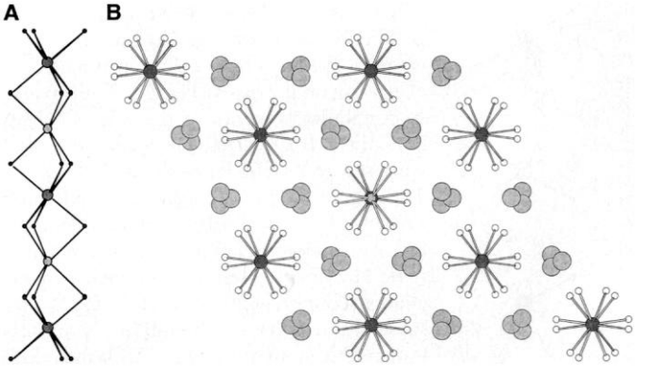

Fig. 1. Structure of Sr_3NiPtO_6. (**A**) One chain showing alternating octahedra and trigonal prisms; (**B**) structure viewed down the *c* axis. Face-sharing MO_6 trigonal prisms alternate with $M'O_6$ octahedra (M = Co, Ni, Zn; M′ = Pt, Ir). These chains are separated by the Sr cations, which maintain charge balance.

T. N. Nguyen and H.-C. zur Loye, Department of Chemistry, Massachusetts Institute of Technology, Cambridge, MA 02139, USA.
P. A. Lee, Department of Physics, Massachusetts Institute of Technology, Cambridge, MA 02139, USA.

*To whom correspondence should be addressed.

2), where M = Co, Ni, Cu, or Zn and M′ = Pt or Ir (*11*, *12*). The structure of these 1D oxides consists of infinite chains of alternating face-sharing MO'_6 octahedra and MO_6 trigonal prisms. The members of this family of oxides exhibit a range of magnetic properties, including 1D antiferromagnetism, ferromagnetism, and a combination of ferromagnetic coupling within the chains and antiferromagnetic coupling between the chains. In particular, we have established that the compositions Sr_3CuPtO_6 (*13*) and Sr_3CuIrO_6 (*14*) (Fig. 2) constitute a 1D Heisenberg antiferromagnet (*11*) and a ferromagnet (*12*), respectively. We reasoned that a solid solution between these two compounds could lead to a system that simultaneously exhibited 1D ferromagnetic and antiferromagnetic coupling along the chains and, therefore, could exemplify a random quantum spin chain paramagnet.

One of the most striking predictions of the theory is that the spin susceptibility, χ, should cross over from the usual high-temperature Curie behavior to a novel low-temperature Curie law, with a Curie constant that depends on P, the probability of finding a ferromagnetic exchange between any two neighboring spins. The limits, $P = 0$ and $P = 1$, correspond to the uniform Heisenberg antiferromagnet and ferromagnet, respectively. The theoretical prediction for the magnetic susceptibility is shown in Fig. 3. In particular, for $P \approx 0.5$, the susceptibility looks almost like that of free spins down to the lowest temperatures, even though exchange interactions lead to an ordering of the spin degree of freedom. This can be understood most easily in the case of classical spins with spin value S_0. As the thermal energy k_BT (where k_B is Boltzmann's constant and T is temperature) falls below the local exchange energy, the spins begin to develop short-range order, with neighboring spins that are parallel or antiparallel, depending on the sign of the exchange interaction. These spins are locked together, forming spin clusters of size $\xi(T)$, which equals the temperature-dependent correlation length of the purely ferromagnetic problem (*6*). We can think of these clusters as forming a large effective spin, S_{eff}. For $P = 0.5$, S_{eff} consists of $\xi(T)$ individual spins of random orientation, and the typical size of S_{eff} is $\sqrt{\xi(T)}\,S_0$. The susceptibility per site attributable to these effective spins is given by

$$\chi = \frac{\mu^2}{3\xi(T)}\frac{\langle S_{eff}^2\rangle}{k_BT} = \frac{\mu^2 S_0^2}{3k_BT} \qquad (1)$$

where μ is the magnetic moment. Note that the temperature-dependent length $\xi(T)$ has canceled out in the expression, and the result is the same as that for free spins.

Detailed analyses have shown that this argument works even in the quantum case with spin S (*9*). For $P = 0.5$, there is a crossover from the high-temperature Curie behavior $\chi = [\mu^2 S(S + 1)]/3k_BT$ to a low-temperature value $\chi = \mu^2 S^2/3k_BT$. As is well known, the $S(S + 1)$ term is a consequence of the quantum nature of the spin operator. Essentially, the effective spin takes on a large value at low temperatures and reaches the classical limit where Eq. 1 applies. This is the main difference between our system and the purely antiferromagnetic random $S = ½$ model, where the ground state remains quantum and is understood as a random collection of spin singlets (*8*).

To create a system containing both ferromagnetic and antiferromagnetic exchange interactions, we decided to prepare a solid solution between the isostructural Sr_3CuPtO_6 and Sr_3CuIrO_6 that would, in a controlled fashion, result in compounds with a range of average exchange values. The solid solution $Sr_3CuPt_{1-x}Ir_xO_6$ represents a good model compound for random spin paramagnetism because it has a total spin between $S = ½$ and $S = 1$, making it an appropriate example of the type of quantum system explained by the theory of Furusaki *et al.*

The solid solution $Sr_3CuPt_{1-x}Ir_xO_6$ ($0 \leq x \leq 1$) was prepared by solid-state synthesis (*15*) and was characterized both structurally (*16*) and magnetically (*17*). Powder x-ray diffraction studies of this solid solution revealed, as expected, diffraction patterns identical to those of the two end members. In the Sr_3CuMO_6 (M = Pt, Ir) structure, which is a distorted version of the Sr_3NiPtO_6 structure, the Cu cations are located in the faces rather than in the centers of the trigonal prisms (Fig. 2). The inverse susceptibility behavior of the solid solution $Sr_3CuPt_{1-x}Ir_xO_6$ (Fig. 4) agrees very well with the theory of Furusaki *et al.* (Fig. 3). The susceptibility of the end member Sr_3CuPtO_6 is well fitted by the Bonner-Fisher expression (*18*) for the antiferromagnetic Heisenberg chain, which yields an exchange coupling $J/k_B = 26.1$ K (*11*). The substitution of Ir into the uniformly antiferromagnetic compound Sr_3CuPtO_6 introduces controllably ferromagnetic interactions into the chains. The Ir ions carry spins $S = ½$, which are coupled ferromagnetically to the neighboring Cu spins (*19*). For example, $Sr_3CuPt_{0.75}Ir_{0.25}O_6$, which contains only a small amount of Ir, contains small ferromagnetic islands separated by antiferromagnetic interactions, whereas $Sr_3CuPt_{0.25}Ir_{0.75}O_6$, which contains a greater amount of Ir, contains large ferromagnetic islands separated by antiferromagnetic interactions. The magnetic behavior of this system follows a systematic trend as a function of the Pt/Ir ratio, which makes it possible to control accurately the high-temperature Weiss constant θ from an antiferromagnetic value of $\theta = -46.6$ K (Sr_3CuPtO_6) to a ferromagnetic value of $\theta = +36.2$ K (Sr_3CuIrO_6).

The system of greatest interest, however, is $Sr_3CuPt_{0.5}Ir_{0.5}O_6$, which contains randomly distributed Pt and Ir sites having random but equal ferromagnetic and antiferromagnetic interactions. The inverse sus-

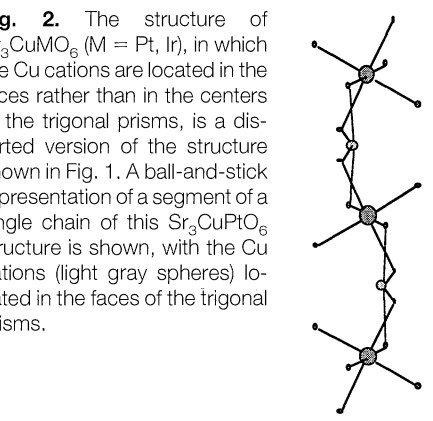

Fig. 2. The structure of Sr_3CuMO_6 (M = Pt, Ir), in which the Cu cations are located in the faces rather than in the centers of the trigonal prisms, is a distorted version of the structure shown in Fig. 1. A ball-and-stick representation of a segment of a single chain of this Sr_3CuPtO_6 structure is shown, with the Cu cations (light gray spheres) located in the faces of the trigonal prisms.

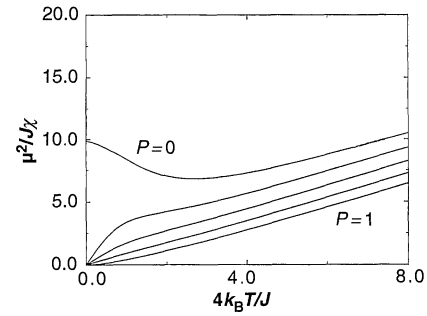

Fig. 3. Theoretical inverse susceptibility for P (or x) = 0, 0.25, 0.5, 0.75, and 1 for the quantum spin chain, as predicted by Furusaki *et al.* (*10*). The limits, $P = 0$ and $P = 1$, correspond to the uniform Heisenberg antiferromagnet and ferromagnet, respectively. As P is increased from 0 to 1, a ferromagnetic component is introduced into the uniformly antiferromagnetic chain. The random quantum spin chain paramagnet is created for $P = 0.5$.

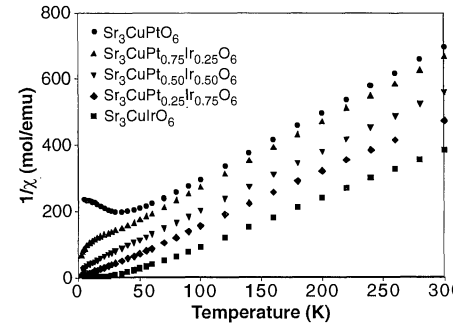

Fig. 4. Inverse susceptibilities for several compositions in the $Sr_3CuPt_{1-x}Ir_xO_6$ solid solution, showing the well-behaved trend of the Weiss constant as a function of the Pt/Ir ratio. Substitution of Ir for Pt enables the controllable introduction of ferromagnetic interactions into the uniformly antiferromagnetic chain. The random quantum spin chain paramagnet is formed for $x = 0.5$.

ceptibility of $Sr_3CuPt_{0.5}Ir_{0.5}O_6$ follows the predicted behavior of a random quantum spin chain (Figs. 3 and 4). At high temperatures, the susceptibility has a linear χ versus $1/T$ dependence and is Curie-like. In this regime, where there is no ordering among unpaired electrons, the spins act independently. A fit of the high-temperature data gave a Weiss constant of $\theta = -12.7$ K and a spin-only moment of $\mu = 2.11$ Bohr magnetons. This moment is in excellent agreement with that expected for a sample containing, on average, one $S = ½$ Cu ion and one-half $S = ½$ Ir ion, which should yield an effective moment of $\mu = 2.12$. At lower temperatures, there is a transition to a regime where spin-spin interactions become important, as indicated by the broad curve in the inverse susceptibility. This transition marks the alignment of spins to form islands of effective spins, as discussed above. Comparison of Figs. 3 and 4 shows that theory and experiment are in good agreement.

REFERENCES AND NOTES

1. F. D. M. Haldane, *Phys. Lett. A* **93**, 463 (1983); *Phys. Rev. Lett.* **50**, 1153 (1983).
2. M. Hase, I. Terasaki, K. Uchinokura, *Phys. Rev. Lett.* **70**, 3651 (1993); Q. J. Harris *et al.*, *Phys. Rev. B* **50**, 12606 (1994).
3. I. S. Jacobs *et al.*, *Phys. Rev. B* **14**, 3036 (1976).
4. R. J. Birgeneau and G. Shirane, *Phys. Today* **31** (no. 12), 32 (1978).
5. L. N. Bulaevskii, A. V. Zvarykina, Y. S. Karimov, R. B. Lyubovskii, I. F. Shchegolev, *Sov. Phys. JETP* **35**, 384 (1972).
6. M. E. Fisher, *Am. J. Phys.* **32**, 343 (1964).
7. D. S. Fisher, *Phys. Rev. B* **50**, 3788 (1994).
8. C. Dasgupta and S. K. Ma, *ibid.* **22**, 1305 (1980).
9. E. Westerberg, A. Furusaki, M. Sigrist, P. A. Lee, *Phys. Rev. Lett.*, **75**, 4302 (1995).
10. A. Furusaki, M. Sigrist, P. A. Lee, K. Tanaka, N. Nagaosa, *ibid.* **73**, 2622 (1994).
11. T. N. Nguyen, D. M. Giaquinta, H.-C. zur Loye, *Chem. Mater.* **6**, 1642 (1994).
12. T. N. Nguyen and H.-C. zur Loye, *J. Solid State Chem.* **117**, 300 (1995).
13. A. P. Wilkinson, A. K. Cheetham, W. Kunnman, A. Kvick, *Eur. J. Solid State Inorg. Chem.* **28**, 453 (1991).
14. M. Neubacher and H. Müller-Buschbaum, *Z. Anorg. Allg. Chem.* **607**, 124 (1992).
15. Polycrystalline samples of Sr_3CuPtO_6, Sr_3CuIrO_6, and $Sr_3CuPt_{1-x}Ir_xO_6$ ($0 < x < 1$) were prepared through solid state reactions. Stoichiometric amounts of $SrCO_3$ (Cerac, 99.5%), Ir metal (Aesar or Engelhard, 99.9%), Pt metal (Aesar, 99.99%), and CuO (Cerac, 99.999%) were intimately mixed with an agate mortar and pestle under acetone and pressed into pellets. The pellets were placed on platinum foil in alumina boats during heating to prevent aluminum contamination. Heating the samples at 1150°C for 2 weeks with intermittent grindings yielded single-phase materials.
16. Powder samples were structurally characterized with a Rigaku RU300 x-ray diffractometer using Cu K_α radiation (wavelength, 1.5405 Å). The oxygen content of the samples was determined by thermogravimetric analysis (TGA) with a Cahn TG121 system. Samples weighing ~50 to ~100 mg were heated to 900°C in 5% H_2:95% N_2. The initial oxygen content was back-calculated from the measured weight loss. Heating oxygen-deficient samples in pure oxygen to 550° to 700°C resulted in a weight gain associated with the complete oxidation of the compounds.
17. Magnetic measurements were obtained with a Quantum Design MPMS superconducting quantum interference device (SQUID) magnetometer at temperatures from 2 to 300 K. All samples were fully oxidized by annealing in O_2 at 550° to 750°C before use in any magnetic measurements. For data collection, all samples were cooled in zero field to 5 K. When the sample temperature reached 5 K, the magnetic field was turned on and data were collected. All data were corrected for the diamagnetic contribution of the calibrated Kel-F sample container.
18. J. C. Bonner and M. E. Fisher, *Phys. Rev.* **135**, 640 (1964).
19. Strictly speaking, in this compound the ferromagnetic bonds always occur in pairs rather than following a random distribution. However, the physical properties of the two models are expected to be similar.

20. Supported in part by NSF Materials Research Science and Engineering Center award DMR 94-00334 and by the MIT Science Partnership Fund.

28 July 1995; accepted 17 November 1995

Th-Pb and U-Pb Dating of Ore-Stage Calcite and Paleozoic Fluid Flow

Joyce C. Brannon,* Susan C. Cole, Frank A. Podosek, Virginia M. Ragan, Raymond M. Coveney Jr., Malcolm W. Wallace, Alison J. Bradley†

Thorium-232–lead-208 and uranium-238–lead-206 radiometric ages for ore-stage calcite show that Mississippi Valley–type (MVT) ore deposits can form in distinct tectonic settings. An age of 251 ± 11 million years for the Jumbo Mine in Kansas, United States, is in agreement with other ages for MVT deposits in the midcontinent of North America. The similarity of ages of these deposits supports the concept that they formed in response to fluid flow during the late Paleozoic Alleghenian-Ouachita orogeny. An age of 351 ± 15 million years for Twelve Mile Bore and Bloodwood-Kapok deposits in Australia indicates that these MVT ores were deposited in a rifting environment.

Analyses of minerals precipitated from or reacted with fluids provide a key means to determine the composition of the parental fluid and the timing of its flow. The minerals that most commonly precipitate in postdepositional sedimentary rocks are carbonates, sulfides, sulfates, silicates, and fluorite. These are also the major components of MVT ore deposits, which are economically important base-metal deposits generally believed to form from warm basinal brines that are not directly associated with igneous activity (*1*).

Radiometric dating of MVT minerals has been difficult because of low abundances of the natural radioactive isotopes useful for isotopic geochronology. Recently, sphalerite and fluorite in MVT ore deposits have been dated successfully by the Rb-Sr and Sm-Nd techniques, respectively (*2–7*). ^{238}U-^{206}Pb has been used to date late-stage gangue calcite (*8*) and early diagenetic calcite (*9*). Here we report ^{238}U-^{206}Pb and ^{232}Th-^{208}Pb data that yield direct ages for ore-stage calcite. The ability to date an additional ore-stage mineral (that is, calcite) provides the means to date many diverse deposits and is especially important for the chronology of MVT ore deposition for which Sangster has noted, "Evaluation of current and future genetic models for MVT deposits depends first and foremost on reliable determinations of the absolute age of ore emplacement" (*10*).

Ore-stage calcite is generally less common

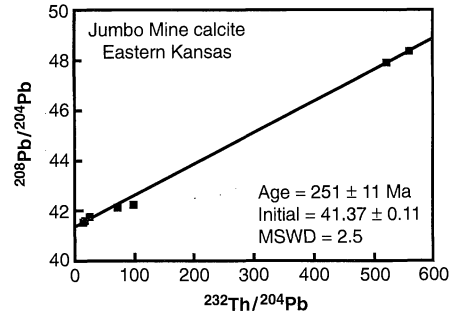

Fig. 1. Th-Pb isochron for ore-stage calcites from the Jumbo Mine, eastern Kansas. Data are from Table 1. Isochron fits were calculated by the York-fit model 1 algorithm of Ludwig (*24*). Ages were calculated for a radioactive decay constant (λ) = 4.9475×10^{-11} year^{-1}. The fit excludes sample JB-8B because the Th value was calculated from a small peak with a rapidly changing background. If JB-8B is included in the regression, the age is 250 ± 22 Ma, and the initial $^{208}Pb/^{206}Pb$ ratio is 41.31 ± 0.19 with a mean standard weighted deviation (MSWD) of 11.

J. C. Brannon, S. C. Cole, F. A. Podosek, Department of Earth and Planetary Sciences and McDonnell Center for the Space Sciences, Washington University, St. Louis, MO 63130–4889, USA.
V. M. Ragan and R. M. Coveney Jr., Department of Geosciences, University of Missouri, Kansas City, MO 64110–2499, USA.
M. W. Wallace and A. J. Bradley, School of Earth Sciences, University of Melbourne, Parkville, Victoria 3052, Australia.

*To whom correspondence should be addressed.
†Present address: Hamersley Iron, Post Office Box 181, Tom Price, Western Australia 6751, Australia.